Neuron
Article

# The Interaction between Stargazin and PSD-95 Regulates AMPA Receptor Surface Trafficking

Cecile Bats,[1] Laurent Groc,[1] and Daniel Choquet[1,*]
[1] Physiologie Cellulaire de la Synapse, UMR 5091 CNRS – Institut François Magendie, Université Bordeaux, Bordeaux 33077, France
*Correspondence: dchoquet@u-bordeaux2.fr
DOI 10.1016/j.neuron.2007.01.030

## SUMMARY

**Accumulation of AMPA receptors at synapses is a fundamental feature of glutamatergic synaptic transmission. Stargazin, a member of the TARP family, is an AMPAR auxiliary subunit allowing interaction of the receptor with scaffold proteins of the postsynaptic density, such as PSD-95. How PSD-95 and Stargazin regulate AMPAR number in synaptic membranes remains elusive. We show, using single quantum dot and FRAP imaging in live hippocampal neurons, that exchange of AMPAR by lateral diffusion between extrasynaptic and synaptic sites mostly depends on the interaction of Stargazin with PSD-95 and not upon the GluR2 AMPAR subunit C terminus. Disruption of interactions between Stargazin and PSD-95 strongly increases AMPAR surface diffusion, preventing AMPAR accumulation at postsynaptic sites. Furthermore, AMPARs and Stargazin diffuse as complexes in and out synapses. These results propose a model in which the Stargazin-PSD-95 interaction plays a key role to trap and transiently stabilize diffusing AMPARs in the postsynaptic density.**

## INTRODUCTION

The AMPA type of ionotropic glutamate receptors (AMPARs) mediates most fast excitatory synaptic transmission in the mammalian central nervous system. They are heterotetrameric structures assembled from combinations of four subunits (GluR1–4; Dingledine et al., 1999; Hollmann and Heinemann, 1994; Keinanen et al., 1990). AMPARs are concentrated at synaptic sites as seen by both electron (Baude et al., 1995; Nusser et al., 1998) and light microscopy as well as electrophysiological recordings (Cottrell et al., 2000). This accumulation has since long been suggested to derive from stabilization by interaction with intracellular scaffold proteins (Braithwaite et al., 2000; Garner et al., 2000; Garner et al., 2002; O'Brien et al., 1998) or extracellular ligands such as Narp (O'Brien et al., 1999). Although a number of proteins have been suggested to be responsible for AMPAR stabilization, the precise identity of the stabilizing molecule(s) has remained elusive.

Over the last decade, constitutive and regulated AMPAR trafficking has been extensively investigated. Biochemical, electrophysiological, and imaging studies have established that AMPARs constitutively and rapidly cycle between the neuronal surface and intracellular compartments through endo- and exocytosis process (Bredt and Nicoll, 2003; Collingridge et al., 2004; Malinow and Malenka, 2002; Song and Huganir, 2002). In addition, single receptor tracking (Borgdorff and Choquet, 2002; Groc et al., 2004; Tardin et al., 2003), fluorescence recovery after photobleaching (FRAP; Ashby et al., 2006), and electrophysiological (Adesnik et al., 2005) approaches have highlighted the contribution of lateral diffusion to AMPAR trafficking. Indeed, using single particle/molecule detection techniques, we previously revealed that individual surface AMPARs diffuse within the plasma membrane of hippocampal neurons and continuously exchange between synaptic and extrasynaptic sites (Borgdorff and Choquet, 2002; Tardin et al., 2003). Thus, the number of AMPARs at synapses results from a dynamic equilibrium between synaptic, extrasynaptic, and intracellular pools of receptors (Triller and Choquet, 2003). Previous work had established that AMPAR endocytosis (Ashby et al., 2006; Blanpied et al., 2002; Racz et al., 2004) and exocytosis (Adesnik et al., 2005; Andrasfalvy and Magee, 2004; Passafaro et al., 2001) likely occurs outside synapses. Altogether, these observations suggest that lateral diffusion could act as a complementary trafficking pathway to exo-/endocytosis for the regulation of AMPAR numbers at synapses. However, the molecular mechanisms involved in controlling receptor lateral diffusion remain unknown.

Over the last years, several AMPAR interacting proteins have been identified. Most of them are cytosolic proteins binding GluR2 C-terminal tail (Barry and Ziff, 2002; Garner et al., 2000; Scannevin and Huganir, 2000; Sheng, 2001). ABP, GRIP, and PICK1 are PDZ-containing proteins that interact with the last four amino acids of GluR2 subunit. Their role in the clustering of AMPARs at synapse and in synaptic plasticity remains unclear. Schematically, ABP/GRIP is concentrated at synaptic plasma membrane or

in intracellular compartments, depending on its palmitoylation (DeSouza et al., 2002). It could thus retain AMPA receptors at these sites. GluR2 phosphorylation by PKC uncouples the receptor from ABP/GRIP anchors (Chung et al., 2000). Phosphorylated AMPARs still bind PICK1 and could be trafficked between synapses and intracellular compartments changing synaptic transmission efficacy (Daw et al., 2000; Perez et al., 2001; Seidenman et al., 2003). More recently, the transmembrane protein Stargazin, also called γ-2, was found to interact directly with AMPAR (Chen et al., 2000). This protein has a PDZ binding site at its C terminus that associates with SAP102, and PSD-95/93 MAGUKs (Chen et al., 2000; Dakoji et al., 2003). Stargazin is spontaneously mutated in Stargazer mice that show absence epilepsy and cerebellar ataxia (Chen et al., 2000). Deficits in cerebellar function of Stargazer are due to a lack of AMPAR in the plasma membrane of cerebellar granule cells. In these cells, expression of full-length Stargazin rescues AMPAR synaptic responses, while expression of Stargazin lacking the PDZ binding site rescues surface delivery but not synaptic clustering of AMPAR, suggesting that the transmembrane protein plays a crucial role at several steps of AMPAR trafficking (Chen et al., 2000). Stargazin belongs to a family of transmembrane AMPAR regulatory proteins which comprise Stargazin, γ-3, γ-4, and γ-8 (Tomita et al., 2003). In the hippocampal pyramidal cells, several TARP isoforms are expressed, leading to the proposal that Stargazin and related TARPS play a similar role in other brain areas (Rouach et al., 2005; Tomita et al., 2003). TARPS are associated with AMPARs early in the synthetic pathway and control their maturation, trafficking, and biophysical properties (Nicoll et al., 2006). First, TARPs are involved in folding and assembly of AMPAR, stabilizing and facilitating their export from the ER (Tomita et al., 2003; Vandenberghe et al., 2005a). Second, Stargazin promotes AMPAR surface expression (Chetkovich et al., 2002; Schnell et al., 2002; Tomita et al., 2003). Third, TARPs are critical for clustering AMPAR at excitatory synapses through their interaction with PSD-95 (Chen et al., 2000; Schnell et al., 2002), a major component of the postsynaptic scaffold (Kim and Sheng, 2004), and probably with other MAGUKs (Elias et al., 2006). PSD-95 overexpression in hippocampal slices enhances specifically synaptic AMPAR-mediated response without changing the number of surface AMPAR. Conversely, Stargazin overexpression increases selectively the number of extrasynaptic AMPAR without changing AMPAR-mediated synaptic currents. These observations indicate that the Stargazin/PSD-95 interaction is involved in the stabilization of AMPARs at synapses. As we and others have previously established that AMPARs can translocate between extrasynaptic and synaptic sites by lateral diffusion, we sought to investigate directly the role of the Stargazin/PSD-95 interaction on the surface trafficking of native and recombinant AMPARs, using single quantum dot tracking and FRAP on live hippocampal neurons.

## RESULTS

### AMPAR Surface Diffusion Is Decreased on PSD-95 Clusters

We first tracked in real time the movement of native GluR1 or GluR2 containing AMPARs at the surface of 7–10 days in vitro (DIV) cultured hippocampal neurons using QDs coupled respectively to antibodies specific for the extracellular N terminus domain of each of these subunits. As previously described (Borgdorff and Choquet, 2002; Groc et al., 2004; Tardin et al., 2003), AMPARs exhibit different patterns of surface diffusion movements ranging from immobile to diffusing freely or within confined domains. We first investigated the relationship between these different types of movement and the localization of AMPARs with respect to PSD-95 clusters. PSD-95 is a major protein of the postsynaptic scaffold (Kim and Sheng, 2004). Accordingly, PSD-95 was endogenously expressed and clustered at excitatory synapses in our cultured hippocampal neurons (see Figure S1 in the Supplemental Data available with this article online). Furthermore, when expressing PSD-95::GFP in neurons, we found that the vast majority of PSD-95::GFP clusters colocalized with v-Glut1 (84% ± 7%), used as a presynaptic marker of glutamatergic synapses, and with Homer 1c::TdimerDsRed, used as a postsynaptic marker (Figure S2). We first quantified the instantaneous diffusion coefficient and the proportion of immobile AMPARs from the whole trajectories. The diffusing properties of AMPARs were similar in control neurons (nontransfected cells) and PSD-95::GFP-expressing neurons. Indeed neither the fraction of immobile receptors (GluR1 control, 51% ± 6%; GluR1 PSD-95::GFP, 51% ± 3%, t test, $p > 0.05$) nor the median diffusion coefficients of mobile receptors (GluR1 control, 0.043 $\mu m^2/s$, IQR [interquartile range] = 0.021–0.083 $\mu m^2/s$; GluR1 PSD-95::GFP, 0.022 $\mu m^2/s$, IQR = 0.008–0.101 $\mu m^2/s$; $p > 0.05$) were significantly different. We generally observed that rapidly diffusing AMPARs located in the extrasynaptic membrane (outside PSD-95 clusters) became less mobile when they reached and colocalized with a PSD-95 cluster, as illustrated in Figure 1 and Movie S1. The mean square displacement (surface explored) of the AMPAR outside the PSD-95 cluster varied linearly with time lag, indicating a freely diffusing pattern of surface diffusion. However, when the same receptor colocalized with a PSD-95 cluster, the MSD-time function was negatively curved, demonstrating that the receptor moved in a confined space (Figures 1A and 1B). In this example, the AMPAR confinement on the PSD-95 cluster was reversible as the receptor exited the cluster after 35 s and recovered a freely diffusing pattern. We then analyzed trajectories according to the membrane localization of the AMPARs (on or outside PSD-95 clusters). Of the total 38 QD-AMPAR complexes that were recorded, eight remained confined on PSD-95::GFP clusters and four alternated between periods of confinement on PSD-95 clusters and periods of free diffusion outside PSD-95 clusters. The fraction of immobile AMPARs (Figure 1D),

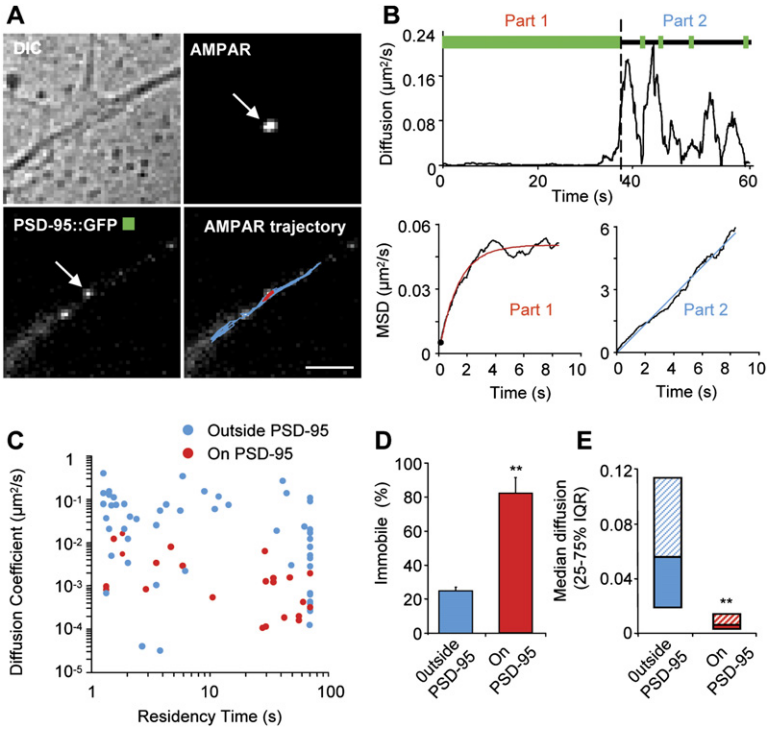


**Figure 1. AMPA Receptor Diffusion Is Reduced on PSD-95 Clusters**

(A) Sample images of a region of a hippocampal pyramidal neuron expressing PSD-95::GFP used for recording the movements of a QD-coupled to GluR1. Top left, DIC image of the region. Top right, image in the fluorescence channel of the QD at a given time point. Bottom left, image in the fluorescence channel of GFP. Bottom right, overlay of a QD trajectory on the PSD-95::GFP fluorescence image. The receptor remains on a PSD-95::GFP cluster (white arrow) for the first 35 s of the recording time (Part 1, in red) and then leaves the cluster and explores the neurite surface (Part 2, in blue). See also Movie S1.

(B) Top, plot of the diffusion versus time for the trajectory represented in (A). The periods of colocalization with PSD-95::GFP clusters are indicated in green lines above the plot, whereas the periods outside PSD-95::GFP clusters are in black. Bottom, plots of the mean square displacement (MSD) versus time for the indicated periods. The MSD calculated for the first part of the trajectory exhibits a negative curvature characteristic of a confined movement whereas the MSD calculated for the second part is linear which is characteristic of a free diffusion. These plots were fitted with either the equation describing confined movement (Kusumi et al., 1993) or with a linear fit.

(C) Plot of the instantaneous diffusion coefficient of QD trajectories versus the time spent inside (red filled circles) or outside (blue open circles) PSD-95::GFP clusters for individual QDs. Trajectories obtained from 38 QDs were cut according to the receptor's location.

(D) Histograms of the mean values ± SEM of the percentage of immobile receptors $D < 3.10^{-3}$ $\mu m^2/s$. The fraction of immobile receptors was higher on PSD-95 clusters (red column, n = 24) than outside (blue column, n = 52), t test, $^{**}p < 0.01$.

(E) The median diffusion (±20%–75% interquartile range) of mobile receptor was decreased on PSD-95::GFP clusters, Mann-Whitney test, $^{**}p < 0.01$. Scale bar, 3 μm.

that we defined as $D_{inst.coef.} < 3.10^{-3}$ $\mu m^2/s$ (the upper limit for measured diffusion coefficient of QDs stuck on glass), was 4-fold higher inside compared to outside PSD-95 clusters (outside PSD-95, 25% ± 2%; on PSD-95, 82% ± 9%; $p < 0.01$) and the median diffusion coefficient of the mobile GluR1-containing AMPARs (Figure 1E) was dramatically reduced on compared to outside PSD-95 clusters (GluR1 outside PSD-95, 0.055 $\mu m^2/s$, IQR = 0.019–0.114 $\mu m^2/s$; GluR1 on PSD-95, 0.007 $\mu m^2/s$, IQR = 0.005-0.014 $\mu m^2/s$; $p < 0.01$). From the MSD curves of confined AMPARs trajectory on PSD-95 clusters, we could measure an explored area of 0.17 μm (SD 0.17, n = 9). It should be noted that not all AMPARs displayed a reduced surface diffusion when colocalized with PSD-95 clusters (Figure 1C). A likely explanation could be that, due to optical resolution limitations, we cannot distinguish whether AMPARs and PSD-95 clusters are strictly apposed, and thus the AMPARs that do not reduce their surface diffusion on PSD-95 clusters may simply be outside such clusters. Otherwise, this could be due to a change in affinity of the AMPAR for the stabilizing scaffold or to a lack of available binding site in the cluster.

## AMPAR Clustering Requires the PDZ Binding Site of Stargazin

In order to investigate the role of Stargazin in the regulation of AMPAR surface movement and distribution, we used either wild-type (WT) or a mutant (ΔC) Stargazin::GFP constructs in which the last C-terminal four amino acids corresponding to the PDZ binding site were removed. When expressed in COS-7 cells, Stargazin WT, but not Stargazin ΔC, allowed PSD-95-induced GluR2 surface clustering (Figure S3). This indicates that the PDZ binding site of Stargazin is required to cluster AMPAR with PSD-95 in heterologous cells.

We first investigated whether Stargazin PDZ binding domain is involved in the synaptic accumulation of AMPARs, as previously indicated (Chen et al., 2000). For this, we measured miniature synaptic currents in neurons transfected for 24–48 hr either with Stargazin WT::GFP or Stargazin ΔC::GFP constructs (Figure 2A). The mEPSC frequency obtained from Stargazin WT neurons was not significantly different from the one obtained in untransfected neurons (untransfected, 1.27 ± 0.19 Hz, n = 13; Stargazin WT, 1.14 ± 0.24 Hz, n = 8; $p > 0.05$), whereas the mEPSC frequency of Stargazin ΔC neurons was

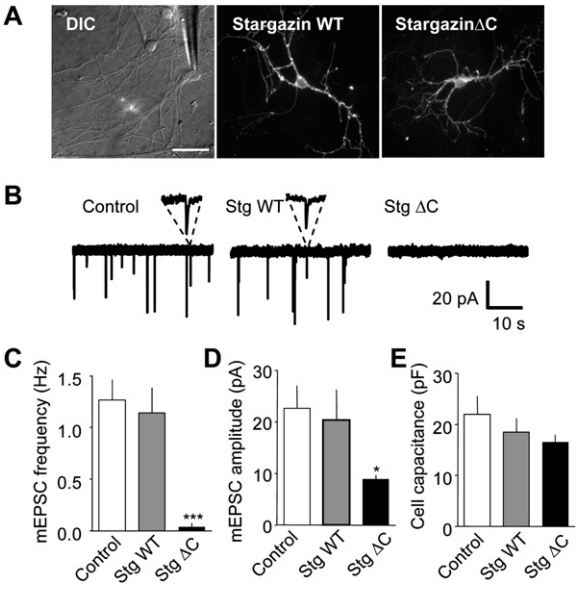


**Figure 2. Stargazin ΔC Reduces Hippocampal Excitatory Synaptic Currents**

(A) Representative control (left panel), Stargazin WT::GFP (center panel)-, and Stargazin ΔC (right panel)-transfected hippocampal cells that were used for electrophysiological recording (see patch pipette in the control panel).

(B) Sample sweeps showing miniature excitatory postsynaptic currents (mEPSCs) recorded at −60 mV in the different conditions. Two individual mEPSC events from control and Stargazin WT neurons are shown in inset.

(C–E) Stargazin ΔC significantly reduces mEPSC frequency (t test, ***$p < 0.001$ when compared to Stargazin WT) and amplitude (D) (t test, *$p < 0.05$ when compared to Stargazin WT), whereas it does not affect the cell capacitance (E) (t test, $p > 0.05$). All values are mean ± SEM; control, n = 13; Stargazin WT, n = 8; Stargazin ΔC, n = 6.

greatly decreased (Stargazin ΔC, 0.04 ± 0.03 Hz, n = 6; $p < 0.001$ compared to untransfected and Stargazin WT; Figures 2B and 2C). The amplitude of the mEPSCs from Stargazin WT-transfected neurons was also not different from the one from untransfected neurons (untransfected, 22.7 ± 4.2 pA, n = 13; Stargazin WT, 20.4 ± 5.8 pA, n = 8; $p > 0.05$). Although Stargazin ΔC neurons have a very low frequency of mEPSCs, providing thus a limited population of all mEPSC events (n = 132), the mEPSC amplitude was significantly decreased in comparison to untransfected neurons (Stargazin ΔC, 8.8 ± 0.7 pA, n = 6; $p < 0.05$; Figure 2D). Regarding the kinetics of the mEPSCs, we found no difference in the half-width between the three groups (untransfected, 1.9 ± 0.1 ms, n = 13; Stargazin WT, 1.6 ± 0.1 ms, n = 8; Stargazin ΔC, 1.9 ± 0.2 ms, n = 6; $p > 0.05$). One possible explanation for the loss of synaptic activity in transfected neurons with Stargazin ΔC is that these neurons lost most of their neurite extensions. An inspection of visualized transfected neurons however indicates that this is very unlikely since these neurons displayed similar shapes as the Stargazin WT ones (Figure 2A). We further measured and compared the cell capacitance of untransfected, Stargazin WT, and Stargazin ΔC neurons in order to obtain an indirect estimation of the cell membrane area. Consistently with the visualization, we found no significant difference in the cell capacitance between neurons (untransfected, 21.9 ± 3.5 pF, n = 13; Stargazin WT, 18.4 ± 2.7 pF, n = 8; Stargazin ΔC, 16.5 ± 1.4 pF, n = 6; $p > 0.05$; Figure 2E). Finally, we ruled out any presynaptic effect of the mutant by measuring similar numbers of FM4-64-stained active synapses in neurons expressing either Stargazin WT or Stargazin ΔC (Figure S4). Thus, these data confirm that the binding of Stargazin to PSD-95 is necessary for a synaptic AMPAR signaling (Chen et al., 2000; Chetkovich et al., 2002; Schnell et al., 2002). Furthermore, by performing an immunostaining of surface AMPARs in neurons expressing Stargazin ΔC, we observed a large decrease in receptor clustering at synaptic sites (Figure S5). All together, these results indicate that the PDZ motif of Stargazin that binds PSD-95 is important for the accumulation of surface AMPARs at synapses.

## AMPAR Diffusion Is Increased at the Surface of Stargazin ΔC-Expressing Neurons

Diffusing surface AMPARs are stabilized on PSD-95 clusters and the binding of Stargazin to its PDZ-containing partners, such as PSD-95, is critical to cluster AMPARs within synapses. The loss of synaptic AMPARs in Stargazin ΔC-expressing neurons could be the result of their surface dispersal outside synapses due to a lack of stabilization in the postsynaptic membrane. To test this hypothesis, we compared the diffusion coefficient distributions of GluR1-containing and GluR2-containing AMPARs from untransfected neighboring neurons (control), Stargazin WT::GFP, and Stargazin ΔC::GFP expressing neurons (Figures 3A and 3B and Figures 3F and 3G). The distributions of the diffusion coefficient from GluR1-containing and GluR2-containing AMPARs were similar. Two main populations can be identified from the bimodal shape of both GluR1 and GluR2 distributions: a mobile fraction ($1.10^{-2} < D_{inst.coef.} < 5.10^{-1}$ $\mu m^2/s$) and a slowly mobile fraction, which is composed of slowly mobile ($D_{inst.coef.} < 1.10^{-2}$ $\mu m^2/s$) and immobile ($D_{inst.coef.} < 3.10^{-3}$ $\mu m^2/s$) AMPARs. In neurons expressing Stargazin WT, there was no significant change in (1) the fraction of immobile receptors (GluR1 control, 52% ± 6%; GluR1 Stargazin WT, 51% ± 5%; $p > 0.05$; GluR2 control, 52% ± 6%; GluR2 Stargazin WT, 48% ± 5%; $p > 0.05$) and (2) the instantaneous diffusion coefficients of both GluR1-containing and GluR2-containing AMPARs (GluR1 control, 0.043 $\mu m^2/s$, IQR = 0.021–0.083 $\mu m^2/s$; GluR1 Stargazin WT, 0.040 $\mu m^2/s$, IQR = 0.015–0.097 $\mu m^2/s$; GluR2 control, 0.054, IQR = 0.018–0.106 $\mu m^2/s$; GluR2 Stargazin WT, 0.059 $\mu m^2/s$, IQR = 0.019–0.095 $\mu m^2/s$; Figures 3C and 3D and Figures 3H and 3I). However, the diffusions of GluR1-containing and GluR2-containing AMPARs at the surface of Stargazin ΔC-expressing neurons were both affected. Indeed, the fraction of immobile GluR1-containing and GluR2-containing AMPARs was significantly decreased when compared to control and

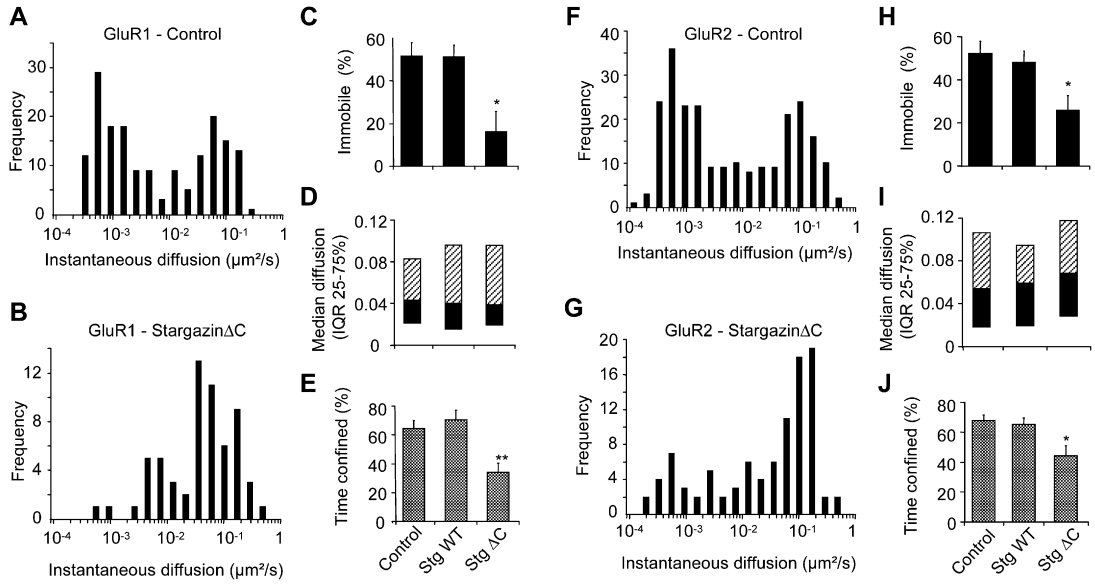


**Figure 3. Overexpression of Stargazin ΔC::GFP Increases the Mobility of GluR1 and GluR2 Subunits in Neuronal Membrane**

(A) Frequency distributions of the diffusions coefficients calculated from the trajectories of GluR1-coupled QDs. Note that they are distributed in two populations. One with $1.10^{-2} < D_{inst.coef.} < 5.10^{-1}$ µm²/s that corresponds to mobile receptors and one with $D_{inst.coef.} < 1.10^{-2}$ µm²/s that corresponds to slowly mobile and immobile ($D_{inst.coef.} < 3.10^{-3}$ µm²/s) receptors.

(B) The proportion of GluR1 with a $D_{inst.coef.} < 1.10^{-2}$ µm²/s in cells expressing Stargazin ΔC::GFP is dramatically decreased compared to neighboring untransfected cells (control, in [A]).

(C) Bar graphs of the mean proportion of immobile receptors ± SEM in the indicated conditions of construct expression. Note that Stargazin ΔC::GFP overexpression (n = 63 QD) induced a decrease in the fraction of immobile receptors compared to either control untransfected neurons (n = 174 QD) or Stargazin WT::GFP (n = 36 QD)-expressing neurons, t test *p < 0.05.

(D) Bar graphs of the median (±20%–75% IQR) diffusions of mobile receptors in the same conditions. Note that the diffusion is statistically unchanged in all conditions, Mann-Whitney test, p > 0.05.

(E) Bar graphs of the mean percentage of time confined ± SEM calculated from trajectories of GluR1-coupled QDs. Note that it is reduced in neurons expressing Stargazin ΔC::GFP compared to control and Stargazin WT::GFP-transfected cells, t test, **p < 0.01.

(F–J) The distribution of GluR2 diffusion coefficients is similar to that of GluR1 (F and G). Stargazin ΔC::GFP (n = 97 QD) overexpression induced a decrease in the proportion ± SEM of immobile GluR2 (H) and in the probability ± SEM to be in a confined state (J) when compared to control (n = 237 QD) or Stargazin WT::GFP (n = 73 QD)-expressing cells, t test, *p < 0.05. There is no change in the median diffusion (±20%–75% IQR) values of mobile receptors between cells expressing either Stargazin WT::GFP or Stargazin ΔC::GFP and control cells (I), Mann-Whitney test, p > 0.05.

Stargazin WT ones (GluR1 Stargazin ΔC, 16% ± 9%; GluR2 Stargazin ΔC, 26% ± 7%; p < 0.05; Figures 3C and 3H), whereas there was no change in the median diffusion coefficient of the mobile GluR1-containing and GluR2-containing AMPARs (GluR1 Stargazin ΔC, 0.039 µm²/s, IQR = 0.019–0.096 µm²/s; GluR2 Stargazin ΔC, 0.068 µm²/s, IQR = 0.028–0.117 µm²/s; p > 0.05; Figures 3D and 3I). These results indicate that Stargazin regulates mainly the immobilization of surface AMPARs rather than their mobility per se. Moreover, the relative percentage of time spent by each AMPAR in a state of confined diffusion dropped in Stargazin ΔC-expressing neurons when compared to control and Stargazin WT-expressing neurons (GluR1 control, 64% ± 6%; GluR1 Stargazin WT, 70% ± 7%; GluR1 Stargazin ΔC, 34 ± 6; p < 0.01; GluR2 control, 68 ± 4; GluR2 Stargazin WT, 65% ± 4%; GluR2 Stargazin ΔC, 44% ± 7%; p < 0.05; Figures 3E and 3J), indicating that Stargazin participates in the confinement of AMPAR in restricted area. In conclusion, AMPAR surface diffusion is modulated by the binding of Stargazin to PDZ-containing scaffold proteins.

## AMPAR Mobility Is Increased at Synaptic Sites by Stargazin ΔC Overexpression

To study the role of Stargazin in regulating AMPAR mobility specifically at synaptic sites, we coexpressed GluR1::HA and Homer 1c::TdimerDsRed together with either Stargazin WT::GFP or Stargazin ΔC::GFP in hippocampal neurons. Homer 1c is a protein of the postsynaptic scaffold and in our experiments Homer 1c::TdimerDsRed is used as a synaptic marker (Okabe et al., 2001; Figure S1). We first measured the diffusion coefficient from whole trajectories. As expected, the fraction of immobile receptors is globally reduced in neurons expressing Stargazin ΔC when compared to neurons expressing Stargazin WT (GluR1 Stargazin WT, 37% ± 9%; GluR1 Stargazin ΔC, 7% ± 3%; p < 0.05), while the median diffusion coefficient of the mobile receptors remains unchanged (GluR1 Stargazin WT, 0.057µm²/s, IQR = 0.027–0.107 µm²/s; GluR1 Stargazin ΔC, 0.055 µm²/s, IQR = 0.021–0.108 µm²/s; p > 0.05). We then analyzed receptor trajectories according to their synaptic (on Homer 1c::TdimerDsRed clusters) or extrasynaptic (outside Homer

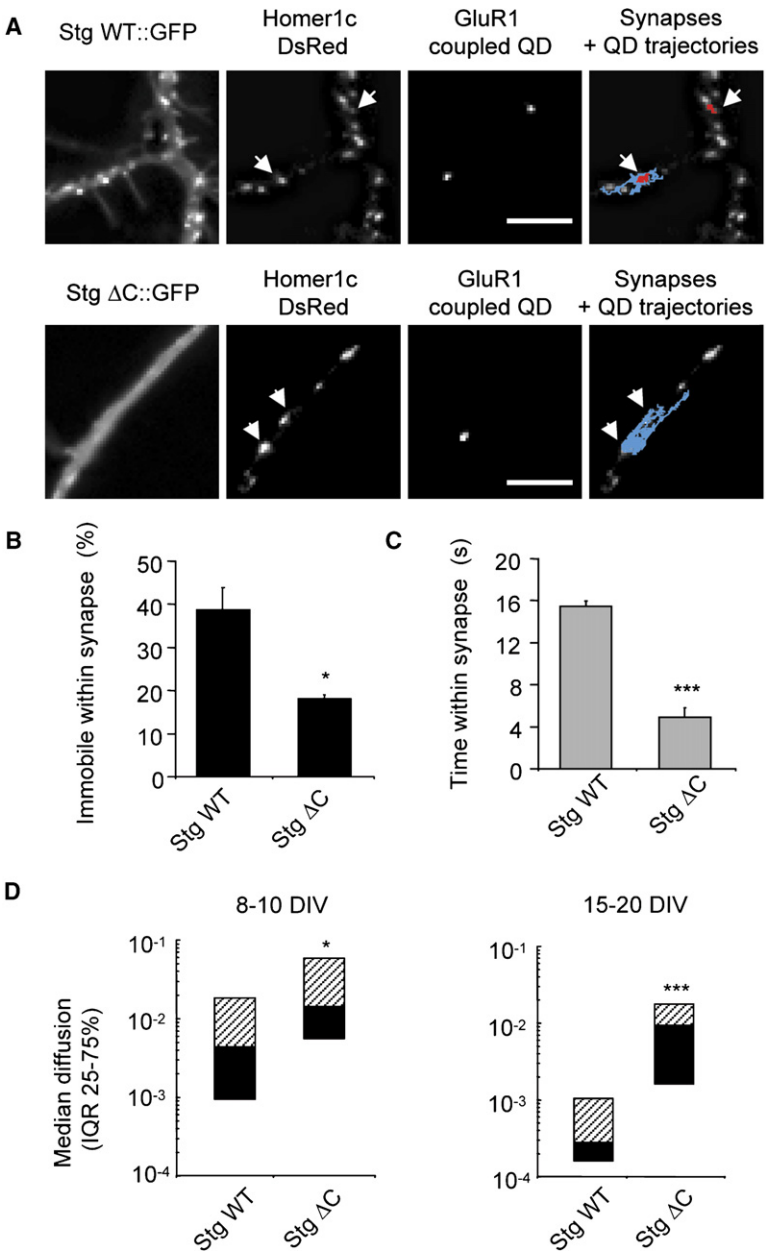


**Figure 4. Stargazin Is Involved in AMPAR Stabilization at Synaptic Sites**

(A) Sample fluorescence images of neurites co-expressing either Stargazin WT::GFP (top panels) or Stargazin ΔC::GFP (bottom panels) together with Homer 1C::TdimerDsRed as a postsynaptic marker and GluR1 subunit tagged with an N-terminal extracellular HA epitope. The various constructs are visualized in separate fluorescence channels, as indicated. The rightmost panels display the overlay of Homer 1c::TdimerDsRed clusters and HA GluR1-coupled QD trajectories. Confined and diffusive periods of movement are shown respectively in red and blue. Homer 1c::TdimerDsRed clusters crossed by the QD during the recording period are marked with white arrows. Scale bar, 5 μm.

(B) Histogram of the mean fraction ± SEM of immobile receptors at synapses in the indicated conditions. Note that it is reduced in neurons expressing Stargazin ΔC (n = 73 QDs) when compared to neurons expressing Stargazin WT (n = 59 QDs), t test, *p < 0.05.

(C) Histogram of time spent by GluR1 at synaptic sites ± SEM. Note that it was decreased 3-fold in cells expressing Stargazin ΔC, t test, ***p < 0.001.

(D) Bar graphs of the median (±20%–75% IQR) diffusions of synaptic GluR1 in young (left graph) and old (right graph) neurons expressing either Stargazin WT::GFP or Stargazin ΔC::GFP. Stargazin ΔC expression induced an increase in diffusion coefficients both in young (n = 31 QDs, Mann-Whitney test, *p < 0.05), and old (n = 39 QDs, Mann-Whitney test, ***p < 0.001) neurons when compared to control values found in Stargazin WT-expressing neurons (young cells, n = 60 QDs; old cells, n = 18 QDs). See also Movie S2.

1c::TdimerDsRed clusters) location. To compare with our previous study (Tardin et al., 2003), we defined three domains in the neuronal membrane: synaptic, extrasynaptic, and juxtasynaptic (an annulus 450 nm around the synapse). As previously, we observed that the proportion of immobile receptors was similar at the periphery of the synapses and in the extrasynaptic membrane (Figure S6). In further analysis, we thus considered only two compartments and merged the juxtasynaptic and extrasynaptic area. When investigating the effect of Stargazin variants, we first found that the fraction of immobile receptors was decreased at both extrasynaptic and synaptic sites in neurons expressing Stargazin ΔC as compared to Stargazin WT (extrasynaptic GluR1 Stargazin WT, 20% ± 5%; extrasynaptic GluR1 Stargazin ΔC, 8% ± 2%; synaptic GluR1 Stargazin WT, 39% ± 5%; synaptic GluR1 Stargazin ΔC, 18% ± 1%; $p < 0.05$; Figure 4B). Second, the median diffusion coefficients of the mobile receptors remained unchanged in all conditions and compartments (extrasynaptic GluR1 Stargazin WT, 0.065 $\mu m^2/s$, IQR = 0.029–0.123 $\mu m^2/s$; extrasynaptic GluR1 Stargazin ΔC, 0.064 $\mu m^2/s$, IQR = 0.032–0.110 $\mu m^2/s$; $p > 0.05$, synaptic GluR1 Stargazin WT, 0.021 $\mu m^2/s$, IQR = 0.007–0.046 $\mu m^2/s$; synaptic GluR1 Stargazin ΔC, 0.026 $\mu m^2/s$, IQR = 0.014–0.055 $\mu m^2/s$; $p > 0.05$; Figure 4C). Third, the amount of time spent by receptors at synapses (Figure 4C) was strongly decreased in cells expressing Stargazin ΔC (synaptic GluR1 Stargazin WT, 15 ± 0.5 s; synaptic

GluR1 Stargazin ΔC, 4.9 ± 0.9 s; $p < 0.001$). Finally, we extended our analysis to older neurons (15–20 DIV). In these neurons, surface AMPARs can be trapped reversibly at spiny synapses (Movie S2; Ashby et al., 2006) showing that the movement of receptors in and out synapses are observed in both young and more mature neurons. On the one hand, the median diffusion coefficient of GluR1 containing synaptic receptors was significantly lower in 15–20 DIV neurons than in 8–10 DIV neurons, as we previously showed for GluR2 (Borgdorff and Choquet, 2002; synaptic GluR1 in old neurons, 0.0003 $\mu m^2/s$, IQR = 0.0002–0.0202 $\mu m^2/s$; synaptic GluR1 in young neurons, 0.004 $\mu m^2/s$, IQR = 0.018–0.001 $\mu m^2/s$; $p < 0.0001$; Figure 4D). On the other hand, Stargazin ΔC overexpression increased GluR1 mobility specifically at synaptic and not extrasynaptic sites (extrasynaptic GluR1 in old neurons expressing Stargazin WT, 0.033 $\mu m^2/s$, IQR = 0.004–0.100 $\mu m^2/s$; extrasynaptic GluR1 in old neurons expressing Stargazin ΔC, 0.042 $\mu m^2/s$, IQR = 0.010–0.123 $\mu m^2/s$; $p > 0.05$, synaptic GluR1 in old neurons expressing Stargazin WT, 0.0003 $\mu m^2/s$, IQR = 0.0002–0.0202 $\mu m^2/s$; synaptic GluR1 in old neurons expressing Stargazin ΔC, 0.009 $\mu m^2/s$, IQR = 0.002–0.018 $\mu m^2/s$; $p < 0.001$). Interestingly, the median diffusion coefficient was similar in young and old neurons in cells expressing the truncation mutant of Stargazin (synaptic GluR1 in young neurons expressing Stargazin ΔC, 0.014 $\mu m^2/s$, IQR = 0.006–0.059 $\mu m^2/s$; $p > 0.05$ compared to GluR1 in old neurons expressing Stargazin ΔC; Figure 4D). Altogether, these results indicate that Stargazin interaction with proteins containing PDZ domains is involved in (1) the immobilization of AMPAR within the synaptic membrane and (2) the developmental increase in AMPARs trapping at synapses, in agreement with the rise in Stargazin (Tomita et al., 2003) and PSD93/95 (Sans et al., 2000) expression during development.

### The PDZ-Binding Site of GluR2 Controls Its Surface Expression but Not Its Lateral Mobility

Given the striking role of Stargazin C terminus in controlling AMPAR surface diffusion, we wondered if AMPAR subunits C termini had any role in controlling surface movements. The direct interaction of GluR2 C terminus with the PDZ-containing proteins ABP/GRIP and PICK1 has been shown to play an important role in the regulation of AMPARs expression at synaptic sites (Collingridge et al., 2004). Whether these proteins are involved solely in modulating the surface expression of the AMPARs or whether they also anchor surface AMPARs at synapse, however, remains unclear. We first used a mutant GluR2, GluR2 ΔC::GFP, in which the last C-terminal four amino acids corresponding to the PDZ binding site were removed. We compared the surface expression of GluR2 ΔC::GFP and wild-type GluR2 WT::GFP in cultured hippocampal neurons. Since the GFP tag is coupled to the extracellular N terminus of GluR2, the surface receptors could be specifically immunolabeled with an anti-GFP. The signal coming from this surface staining was normalized to that of the signal of the GFP, which corresponds to the total intracellular and surface expression of the recombinant protein. GluR2 surface expression was reduced by half when its PDZ binding site was deleted (GluR2 WT, 3.3% ± 0.5%; GluR2 ΔC, 1.5% ± 0.3%; $p < 0.05$; Figures 5A and 5B). Using Homer 1c::TdimerDsRed as a postsynaptic marker, we observed that both GluR2 WT::GFP and GluR2 ΔC::GFP nevertheless colocalized with Homer 1c (Figure 5B). Therefore, GluR2 ΔC::GFP is less expressed at the neuronal membrane but is still clustered at excitatory synapses.

To investigate the role of GluR2 PDZ interactors in controlling GluR2 lateral mobility, we tracked in real time the movement of GluR2 WT::GFP or GluR2 ΔC::GFP at the neuronal surface using QDs coupled to anti-GFP. The diffusing properties of GluR2 were not significantly changed by the deletion of the PDZ binding site. Indeed, the fraction of immobile receptors (Figure 5C) and the median diffusion coefficients of mobile receptors (Figure 5D) were similar for GluR2 WT::GFP and GluR2 ΔC::GFP (percentage of immobile—GluR2 WT, 48% ± 4%; GluR2 ΔC, 58% ± 10%; $p > 0.05$; median diffusion coefficients—GluR2 WT, 0.046 $\mu m^2/s$, IQR = 0.016–0.089 $\mu m^2/s$; GluR2 ΔC, 0.034 $\mu m^2/s$, IQR = 0.013–0.071 $\mu m^2/s$; $p > 0.05$). Moreover, the percentage of time spent by the receptor in confined state was unchanged by the mutation (GluR2 WT, 64% ± 5%; GluR2 ΔC, 68% ± 7%; $p > 0.05$).

We analyzed receptor movements according to their synaptic (on Homer 1c::TdimerDsRed clusters) or extrasynaptic location (outside Homer 1c::TdimerDsRed clusters). We did not detect any difference between GluR2 WT::GFP and GluR2 ΔC::GFP diffusion within synapses, neither in the fraction of immobile receptors (extrasynaptic GluR2 WT, 31% ± 8%; extrasynaptic GluR2 ΔC, 51% ± 8%; synaptic GluR2 WT, 78% ± 7%; synaptic GluR2 ΔC, 84% ± 5%; $p > 0.05$; Figure 5E) nor in the median diffusion coefficients of mobile receptors (extrasynaptic GluR2 WT, 0.043 $\mu m^2/s$, IQR = 0.021–0.089 $\mu m^2/s$; extrasynaptic GluR2 ΔC, 0.041 $\mu m^2/s$, IQR = 0.013–0.079 $\mu m^2/s$; synaptic GluR2 WT, 0.014 $\mu m^2/s$, IQR = 0.008–0.138 $\mu m^2/s$; synaptic GluR2 ΔC, 0.008 $\mu m^2/s$, IQR = 0.004–0.031 $\mu m^2/s$; Mann-Whitney test, $p > 0.05$). Furthermore, the mean time spent within synapses was unchanged by the deletion of the PDZ-binding motif (synaptic GluR2 WT, 20 ± 4 s; synaptic GluR2 ΔC, 16 ± 4 s; $p > 0.05$; Figure 5F). In order to confirm these results on native GluR2 containing AMPA receptors, we used the C-terminal SVKI peptide of GluR2 fused to the membrane permeant TAT sequence to compete for the binding of GluR2 to its partner scaffold proteins, as previously established (e.g., Daw et al. [2000], Kim et al. [2001], Terashima et al. [2004]). In the presence of SVKI peptide, both the percentage of immobile native GluR2 and the median diffusion of the mobile receptors were similar to those measured in matched control experiments with a scrambled peptide (Figure S7).

Altogether, these results show that, in resting conditions, PDZ proteins interacting with GluR2 C terminus

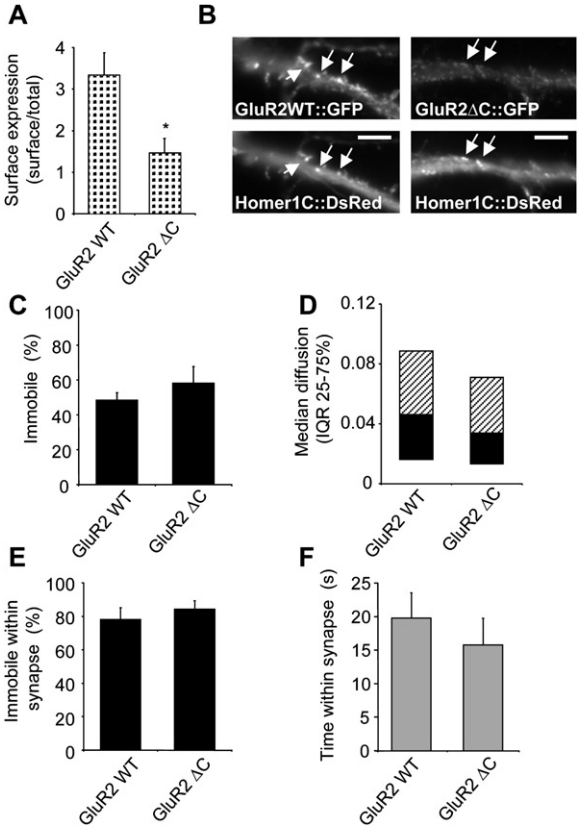


**Figure 5. The Interaction of GluR2 C Terminus with PDZ Domain-Containing Proteins Is Involved in GluR2 Surface Expression but Not in Its Stabilization at Synaptic Sites**

(A) The expression of GluR2 ΔC::GFP at the surface of hippocampal neurons is reduced when compared to GluR2 WT::GFP ; t test, *$p < 0.05$ (n = 8 neurons for each condition). Surface receptors were detected with anti-GFP immunostaining normalized to total GFP fluorescence levels.

(B) Sample fluorescence images of neurites coexpressing either GluR2 WT::GFP (left panels) or GluR2 ΔC::GFP (right panels) together with Homer 1c::TdimerDsRed as a postsynaptic marker. The top panels correspond to an anti-GFP immunostaining of surface GluR2. Anti-GFP was revealed with a Cy5 coupled-secondary antibody. Scale bar, 10 μm. Note that GluR2 ΔC::GFP can be clustered at synaptic sites like GluR2 WT::GFP. Some GluR2 clusters colocalized with Homer 1c::TdimerDsRed clusters are marked with white arrows.

(C) Histograms of the mean ± SEM percentage of immobile receptors. The fractions of immobile receptors obtained from either GluR2 WT::GFP (n = 107)- or GluR2 ΔC::GFP (n = 87)-coupled QDs trajectories were not significantly different, t test, $p > 0.05$.

(D) Bar graphs of the median (±20%–75% IQR) diffusions of mobile receptors in the same conditions. Note that again the diffusion is statistically unchanged in all conditions, Mann-Whitney test, $p > 0.05$.

(E) Histogram of the mean ± SEM percentage of immobile receptors at synaptic sites. The fraction of immobile receptors at synapses is similar in neurons expressing GluR2 ΔC::GFP and in neurons expressing GluR2 WT::GFP, t test, $p > 0.05$.

(F) Histogram of the mean ± SEM time spent by GluR2 WT::GFP or GluR2 ΔC::GFP at synaptic sites. The percentage of time spent within synapse is not changed by the deletion of GluR2 PDZ-binding site, t test, $p > 0.05$.

are mainly involved in the regulation of GluR2 surface expression but not in its trapping at synaptic sites. The GluR2 PDZ-binding motif could be either required for AMPAR retention in plasma membrane (Osten et al., 2000) or for receptor recycling at the surface (Passafaro et al., 2001).

## AMPAR Surface Diffusion Is Modulated by PSD-95/Stargazin Interaction

To specifically investigate whether the PSD-95/Stargazin interaction modulates AMPAR surface diffusion, we used PSD-95/Stagazin compensatory mutants where the interaction between the PDZ domain and its ligand is converted from class I to class II (Schnell et al., 2002). Schematically, the Stargazin mutant (StargazinT321F) can only interact with the compensatory mutant of PSD-95 (PSD-95H225V) and not with the native PSD-95. We first tested the validity of the constructs by expressing StargazinT321F::GFP alone. It displayed a uniform distribution and did not coaggregate with v-Glut1 clusters. However, expression of both StargazinT321F::GFP and PSD-95H225V relocated StargazinT321F::GFP clusters to synaptic sites (Figure S8). Thus, as previously shown (Schnell et al., 2002), the synaptic targeting of Stargazin is dependent on the presence of synaptic PSD-95. Regarding the regulation of GluR2-containing AMPAR surface trafficking, we found that the fraction of immobile receptors was dramatically reduced in StargazinT321F-expressing neurons when compared to control and most importantly to StargazinT321F/PSD-95H225V-expressing neurons (GluR2 control, 76% ± 12%; GluR2 StargazinT321F = 10% ± 6%; GluR2 StargazinT321F + PSD-95H225V = 69% ± 7%; $p < 0.01$; Figure 6B). The diffusion coefficient of the mobile GluR2-containing AMPARs was not significantly affected in all of the conditions, consistent with a role of the Stargazin/PSD-95 interaction in the immobilization of surface GluR2-containing AMPARs rather than in the receptor mobility (GluR2 control, 0.045 $\mu m^2/s$, IQR = 0.014–0.093 $\mu m^2/s$; GluR2 StargazinT321F, 0.080 $\mu m^2/s$, IQR = 0.031–0.131 $\mu m^2/s$, GluR2 StargazinT321F + PSD-95H225V, 0.043 $\mu m^2/s$, IQR = 0.024–0.0812 $\mu m^2/s$; $p < 0.05$). Moreover, the relative time spent by each AMPAR in a confined pattern was significantly reduced in StargazinT321F-expressing neurons when compared to StargazinT321F/PSD-95H225V-expressing neurons (GluR2 control, 84% ± 6%; GluR2 StargazinT321F = 41% ± 7%; GluR2 StargazinT321F + PSD-95H225V = 78% ± 5%; $p < 0.01$; Figure 6C). Similar results for the surface trafficking were obtained for GluR1-containing AMPARs (data not shown). As expected the mobility of the receptors was changed on StargazinT321F/PSD-95H225V clusters (Figures 6D and 6E), immobilization being increased (GluR2 outside StargazinT321F/PSD-95H225V, 37% ± 6%; GluR2 on StargazinT321F/PSD-95H225V, 77% ± 10%; $p < 0.01$) and median diffusion being reduced (GluR2 outside StargazinT321F/PSD-95H225V, 0.060 $\mu m^2/s$, IQR = 0.028–0.114 $\mu m^2/s$; GluR2 on StargazinT321F/PSD-95H225V, 0.013 $\mu m^2/s$, IQR = 0.005–0.032

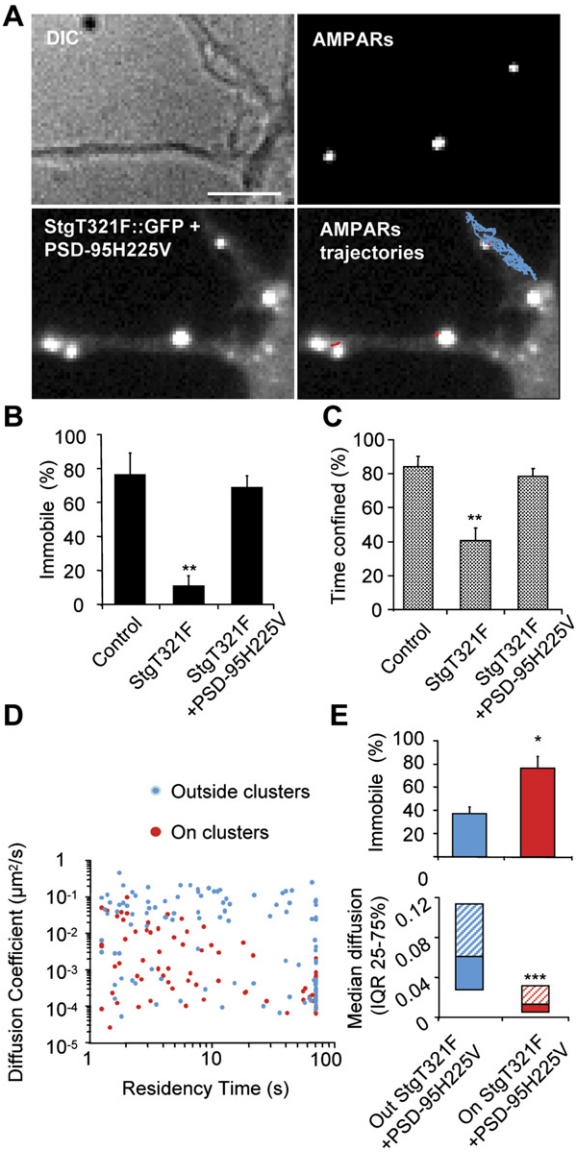


**Figure 6. Stargazin Stabilizes AMPAR in Neuronal Membrane through Its Specific Interaction with PSD-95**

Neurons were transfected with either StargazinT321F::GFP alone or StargazinT321F::GFP and the compensatory mutant PSD-95H221V.

(A) Sample images of the same neuritic field visualized by DIC (top left) and in the fluorescence channel of StargazinT321F::GFP (bottom left) or of GluR2-coupled QDs (top right). In this field, three QDs coupled to GluR2 subunits are seen in a neuron where StargazinT321F::GFP clustering was rescued by PSD-95H221V expression. The bottom right panel represents the overlay of StargazinT321F::GFP clusters and QDs trajectories (confined and diffusive movements are shown respectively in red and blue). Scale bar, 5 μm.

(B and C) Histograms of the mean fraction ± SEM of immobile receptors (B) and of the mean percentage ± SEM of time spent in a confined state (C) in the indicated conditions of transfection. Note that StargazinT321F::GFP overexpression (n = 40 QD) induces a significant reduction of the immobile receptors fraction and in the percentage of time spent in a confined state compared to the values obtained in nontransfected neighboring neurons (n = 48 QD), t test, **p < 0.01. Coexpression of PSD-95 H221V with StargazinT321F::GFP (n = 88 QD) rescues both immobilization and confinement of the receptors in the membrane.

(D) Plot of the instantaneous diffusion coefficients of portions of receptor trajectories versus the time spent on (red circles) or outside (blue circles) StargazinT321F::GFP clusters in cells coexpressing StargazinT321F::GFP and PSD-95H221V. Trajectories were cut according to the receptor's location.

(E) Top, mean fraction ± SEM of immobile receptors outside (blue bars) and inside (red bars) StargazinT321F::GFP clusters. t test, *p < 0.05. Bottom, median diffusion (±20%–75% IQR) of mobile receptors outside (blue bars) and inside (red bars) StargazinT321F::GFP clusters. Mann-Whitney test, ***p < 0.001.

$\mu m^2/s$; $p < 0.001$). Thus, these results indicate the critical role of the specific interaction between Stargazin and PSD-95 in stabilizing AMPAR in neuronal membrane.

## Stargazin and AMPA Receptors Diffuse as Complexes in the Neuronal Membrane

We then investigated the dynamic of AMPAR/Stargazin/PSD-95 complexes. Using anti-HA-coupled QD, we first followed Stargazin surface movements in neurons coexpressing Stargazin::HA and PSD-95::GFP and measured Stargazin diffusion according to its localization with respect to PSD-95 clusters. Freely diffusing extrasynaptic Stargazin was reversibly stabilized on PSD-95::GFP clusters (Figure 7A and Movie S3). Accordingly, on PSD-95 clusters, the fraction of immobile Stargazin was increased (Stargazin outside PSD-95::GFP, 20% ± 4%; Stargazin on PSD-95::GFP, 73% ± 10%; $p < 0.01$; Figure 7B), and the median diffusion of mobile Stargazin was decreased (Stargazin outside PSD-95::GFP, 0.070 $\mu m^2/s$, IQR = 0.035–0.116 $\mu m^2/s$; Stargazin on PSD-95::GFP, 0.015 $\mu m^2/s$, IQR = 0.005–0.035 $\mu m^2/s$; $p < 0.01$; Figure 7C). It should be noted that the diffusion properties of Stargazin were modified on PSD-95 clusters to the same extent as those of AMPARs.

However, AMPAR could diffuse out of synapses due to unbinding from Stargazin or to unbinding of Stargazin from PSD-95. To distinguish between these alternatives, we studied the effect of crosslinking induced GluR2 immobilization on Stargazin::GFP diffusion using FRAP. Neurons were cotransfected with Stargazin::GFP and an extracellularly TdimerDsRed-tagged GluR2. We incubated neurons with excess anti-DsRed antibody to specifically crosslink GluR2::TdimerDsRed. Such a treatment immobilizes surface expressed AMPARs (data not shown and Ashby et al. [2006]). For FRAP analysis, we selected two types of regions, containing either scattered or clustered Stargazin::GFP. Stargazin clusters are most likely synaptic, 76% ± 3% of them being colocalized with Homer 1c::TdimerDsRed (data not shown). We first measured the recovery of the fluorescence signal after the photobleaching of Stargazin::GFP in control condition (without antibody). Consistent with the results obtained with single quantum dots tracking, the fluorescence recovery was slower (half decay time control values; Figure 8C) and occurred to a lower extent (mobile fraction control values;

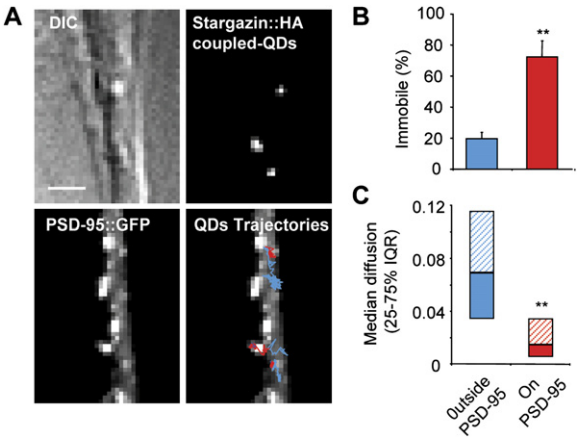


**Figure 7. Stargazin Diffusion Is Reduced on PSD-95 Clusters**

(A) Sample images of a neurite coexpressing PSD-95::GFP and Stargazin WT tagged with an N-terminal extracellular HA epitope. The neurite is visualized by DIC (top left) and in the fluorescence channel of PSD-95::GFP (bottom left) or of Stargazin WT::HA-coupled QDs (top right). The bottom right panel displays the overlay of PSD-95::GFP clusters and Stargazin::HA-coupled QDs trajectories. Confined and diffusive periods of movement are shown respectively in red and blue. Scale bar, 2 μm. See also Movie S3.

(B) Histograms of the mean values ± SEM of the percentage of immobile Stargazin. The fraction of immobile Stargazin was higher on PSD-95 clusters (red column, n = 11) than outside (blue column, n = 137), t test, $^{**}p < 0.01$.

(C) The median diffusion (±20%–75% IQR) of mobile Stargazin was decreased on PSD-95::GFP clusters, Mann-Whitney test, $^{**}p < 0.01$.

Figure 8B) in areas of clustered (i.e., synaptic) than scattered (i.e., extrasynaptic) Stargazin. This further indicates that both the mobile fraction and the diffusion coefficient of Stargazin were reduced at synaptic sites. We then measured Stargazin::GFP fluorescence recovery after preincubation with anti-GluR2::TdimerDsRed antibodies. This treatment induced a higher clustering of Stargazin at synaptic sites (data not shown) and significantly reduced the fraction of mobile clustered Stargazin. Even more interestingly, GluR2 crosslinking modified both the fraction of mobile and the recovery time of scattered (extrasynaptic) Stargazin. As a control, this treatment did not change the diffusion properties of a control GFP-coupled membrane protein (NrCAM-TM::GFP, see Experimental Procedures; Falk et al. [2004]) that does not associate with AMPARs (Figure S9). Altogether, these data strongly suggest that AMPAR and Stargazin diffuse as complexes in both synaptic and extrasynaptic plasma membrane.

## DISCUSSION

AMPA receptors can exchange between synaptic and extrasynaptic compartments by lateral diffusion in the neuronal membrane (Ashby et al., 2006; Borgdorff and Choquet, 2002; Groc et al., 2004; Tardin et al., 2003). In this study, we identified a molecular interaction strikingly involved in the concentration of diffusing AMPAR at synaptic sites. We showed, using single quantum dot imaging and FRAP in live hippocampal neurons, that AMPARs diffuse in the neuronal membrane together with Stargazin and are trapped reversibly at synapses through the specific binding of Stargazin to the PDZ-domain scaffold protein PSD-95. The disruption of the interaction between Stargazin and PSD-95 strongly increased AMPAR surface diffusion, removing AMPARs from postsynaptic sites as further demonstrated by the large reduction of the basal excitatory synaptic transmission. In contrast, the C-terminal domain of GluR2 does not seem to be involved in controlling AMPAR lateral diffusion. These results shine new light on how Stargazin modulates AMPARs trafficking and further strengthen a model in which TARPs are essential partners of AMPARs for their stabilization at synaptic sites.

### QD-Based Tracking of Surface AMPARs and PSD-95

The surface diffusion of AMPARs has previously been described using single particle (Borgdorff and Choquet, 2002; Groc et al., 2004; Howarth et al., 2005) and molecule (Groc et al., 2004; Tardin et al., 2003) tracking, FRAP (Ashby et al., 2006), and more recently using an electrophysiological approach with a photoactivable membrane-impermeable AMPAR antagonist (Adesnik et al., 2005). Although each approach has its own advantages and drawbacks (Cognet et al., 2006), the use of individual nanometer-sized fluorescent objects, the quantum dots, uniquely allows the tracking of individual or small assemblies of surface AMPARs for long recording period in rather confined space (e.g., the synaptic cleft) (Dahan et al., 2003; Groc et al., 2004). Furthermore, it provides a way to characterize the diffusion of a receptor and measure the time spent by this receptor in a specific compartment, i.e., extrasynaptic and synaptic membranes. We found that a significant fraction of GluR1- and GluR2-containing AMPARs laterally exchange between the extrasynaptic and postsynaptic membranes. We investigated the role of PSD-95 on AMPAR stabilization because PSD-95 expression enhances postsynaptic clustering of glutamate receptors (El-Husseini et al., 2000; Schnell et al., 2002) and plays, more generally, a key role during AMPAR-mediated synaptic transmission and plasticity (Beique and Andrade, 2003; Beique et al., 2006; Ehrlich and Malinow, 2004; Elias et al., 2006; Stein et al., 2003). Moreover, a very recent study using short hairpin RNAs to acutely knock down PSD-95 expression showed that PSD-95, together with PSD-93, is involved in synaptic targeting of AMPARs (Elias et al., 2006). While previous work on a PSD-95 KO mouse reported enhanced long-term potentiation and impaired learning in mice with mutant postsynaptic density-95 protein (Migaud et al., 1998), the interpretation of these data are, however, complicated by the fact that these PSD-95 KO mice still express, albeit at low levels, a functional truncated form of PSD-95 (Ehrlich and Malinow, 2004; Schnell et al., 2002). In contrast, AMPAR-mediated transmission is defective in mice with

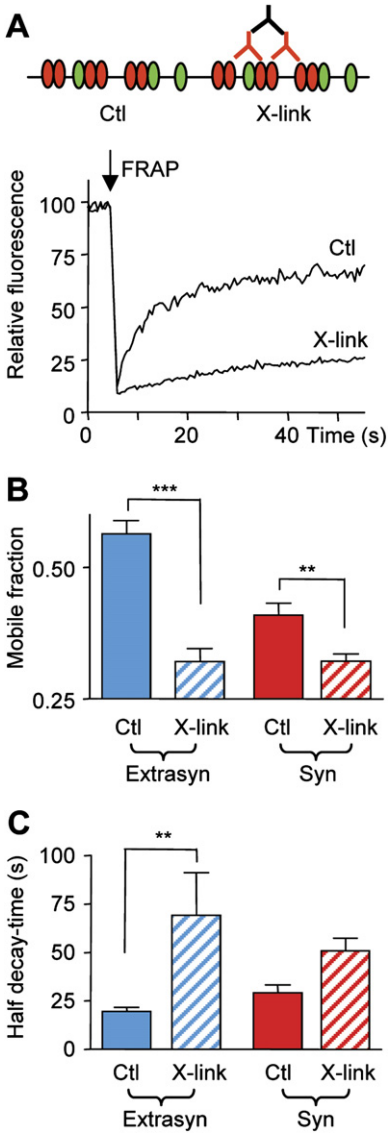


**Figure 8. Stargazin and AMPARs Diffuse as Complexes in the Synaptic and Extrasynaptic Membrane**

(A) Top, scheme describing the experimental strategy to determine if AMPA receptors and Stargazin diffuse as complexes in the neuronal plasma membrane. GluR2::TdimerDsRed was cotransfected with Stargazin WT::GFP. Surface GluR2 was specifically crosslinked by successive addition of an anti-TdimerDsRed and a Cy5-coupled secondary antibody ("X-linked" condition). Bottom, plots of the normalized fluorescence intensity of Stargazin WT::GFP versus time before and after photobleaching (vertical arrow), recorded in control condition without any antibody or in conditions of GluR2 crosslinking (X-linked). Note that the GFP fluorescence recovery was lower when GluR2 was crosslinked.

(B) Histogram of the mean ± SEM Stargazin::GFP mobile fraction for regions containing either scattered extrasynaptic (in blue) or clustered synaptic (in red) Stargazin. Note that the fraction of mobile Stargazin was lower at synaptic than in extrasynaptic membrane in control condition and was decreased at both synaptic and extrasynaptic sites in X-linked condition.

(C) Histogram of the mean ± SEM half-recovery times in the same conditions. Fluorescence recovery was significantly slower at extrasynaptic sites in X-linked condition.

a complete PSD-95 gene deletion (Beique et al., 2006). These data are in perfect accordance with our hypothesis on the key role of the Stargazin-PSD-95 interaction in controlling AMPAR stabilization at synapses. Accordingly, diffusing AMPARs were stabilized on PSD-95 clusters and this process was only transient (in the order of tens of seconds). Some of the AMPARs colocalized with PSD-95 clusters were still mobile, their movement being however strongly confined to areas of few hundreds of nanometer. This may represent either rapid binding/unbinding of the AMPAR/Stargazin complex to scaffold, i.e., PSD-95, elements or confinement of the movement of AMPAR/Stargazin/PSD-95 complex within the dense matrix of the postsynaptic density. AMPARs that are not stabilized on PSD-95 clusters mostly displayed free Brownian movements, whether extrasynaptic or in the presence of mutant forms of Stargazin. This shows that in the absence of a stabilizing interaction, AMPARs can travel long distances and possibly exchange between synaptic sites. Altogether, this indicates that the organization of surface AMPARs within synapses is highly dynamic since it relies on an equilibrium between diffusive and stabilized states of the receptors (Choquet and Triller, 2003). Interestingly, such view of the postsynaptic organization is not restricted to AMPARs since diffusing mGluR5 and glycine receptors can also be stabilized at the surface by the postsynaptic scaffold proteins homer and gephyrin, respectively (Meier et al., 2001; Serge et al., 2002), indicating that receptor trapping by scaffold proteins represents a general process to stabilize and accumulate surface receptors within the postsynaptic membrane.

It should be noted that a fraction of immobile AMPARs was not localized on PSD-95 clusters, possibly due to the existence of a small subset of synapses that lack PSD-95 but express the Stargazin interacting protein PSD-93, as seen in vivo (Elias et al., 2006). Consistently, we observed few excitatory terminals not associated with a PSD-95 immunostaining (see Figure S1), but we could not explore this heterogeneity further in our cultured hippocampal neurons since the anti-PSD-95 antibody (clone 7E3-1B8) we used slightly crossreacts with PSD-93 (Sans et al., 2000).

## AMPAR Surface Trafficking in Stargazin ΔC-Expressing Neurons

None of the AMPAR subunits bind directly PSD-95. Among the several postsynaptic proteins that interact with AMPARs and which then may serve a link to PSD-95, Stargazin and the other members of the TARP family have emerged as key partners for AMPAR trafficking (Nicoll et al., 2006). Stargazin overexpression increases selectively the number of extrasynaptic AMPARs without changing AMPARs mediated synaptic currents, but its

interaction with PSD-95 is critical for clustering AMPARs at excitatory synapses (Chen et al., 2000; Schnell et al., 2002). Based on the present data, we further propose that the loss of synaptic AMPARs in Stargazin ΔC-expressing neurons is the result of their surface dispersal outside synapses due to a lack of stabilization in the postsynaptic membrane. The use of PSD-95 and Stargazin compensatory mutants, in which StargazinT321F can only interact with the compensatory mutant PSD-95H225V, demonstrated that the Stargazin/PSD-95 interaction is important to restrict the surface diffusion of AMPARs and thus to confine them on PSD-95 synaptic clusters. Consistent with the fact that Stargazin binds all known GluR subunits (Chen et al., 2000), the disruption of the Stargazin/PSD-95 interaction affected equally the surface trafficking of GluR1- and GluR2-containing AMPARs.

In the presence of Stargazin mutants that do not bind PSD-95, most AMPARs displayed rapid free diffusion, similar to that observed for freely diffusing extrasynaptic AMPARs in control conditions. These Stargazin mutants likely compete for endogenous TARPs for binding to AMPARs, thus promoting the formation of AMPAR/mutant Stargazin complexes that cannot be stabilized on PSD-95 clusters. This further suggests that the Stargazin/AMPAR complex can diffuse freely in the membrane in the absence of interaction with PSD-95. However, a small fraction of AMPARs still exhibited confined diffusion or even immobilization in the presence of mutant Stargazin, suggesting the existence of different interactors for membrane stabilization. Several possibilities can be discussed. First, confined events observed in neurons expressing Stargazin mutants could correspond to corralling of AMPAR surface diffusion within generic membrane domains created by extracellular matrix and/or cytoskeleton fences (Kusumi et al., 2005). Second, a subset of AMPARs could still be bound to endogeneous TARPs. Indeed, several TARP isoforms in addition to Stargazin are expressed in hippocampal pyramidal neurons (Tomita et al., 2003). γ-8, which has a high sequence homology with Stargazin, is enriched in hippocampus, in which the expression of the other Stargazin-related proteins γ-2, γ-3, and γ-4 is also observed (Tomita et al., 2003). All of these proteins can rescue AMPAR response in Stargazer cerebellar granule cells (Tomita et al., 2003). Along this line, it is interesting to note that in γ-8 KO mice, the total, as well as the extrasynaptic pools, of AMPARs are greatly reduced, while synaptic AMPARs are only decreased by 35%. The synaptic AMPAR response is further reduced in γ-8 γ-2 double-KO mice, supporting the proposal that several hippocampal TARPs contribute to the synaptic targeting of AMPARs (Rouach et al., 2005). Thus, in our experiments, it is possible that interactions between AMPAR and endogenous TARPs remain in spite of Stargazin mutant overexpression. This may explain the remaining fraction of immobile surface AMPARs. Third, other scaffolding proteins, such as SAP-97 or NSF, interact with specific AMPAR subunits (Collingridge et al., 2004) and may thus serve as scaffold in the absence of Stargazin. However, as previously pointed out, the remaining immobile fraction was similar for GluR1- and GluR2-containing AMPARs, suggesting a rather unspecific effect on the AMPAR subunit type. Fourth, the neuronal pentraxin NARP and NP1 are enriched at excitatory synapses (O'Brien et al., 1999; Xu et al., 2003) and interact directly with all of the four AMPAR subunits inducing AMPARs surface clustering (O'Brien et al., 1999, 2002; Xu et al., 2003). NARP and NP1 could thus act as AMPARs stabilizing extracellular factors. Finally, we cannot rule out that a proportion of these immobile AMPARs are trapped on clathrin-coated pits or recently internalized (Groc et al., 2004; Tardin et al., 2003).

It should be noted that we observed immobile receptors at extrasynaptic sites (outside Homer 1c::TdimerDsRed clusters), some of them being released by Stargazin ΔC expression. These receptors could be trapped by extrasynaptic clusters of PSD-95 or other MAGUKs interacting with Stargazin such as SAP-102 and PSD-93. Indeed, we found that 8% ± 3% of PSD-95::GFP clusters were not colocalized with Homer 1c::TdimerDsRed. Such extrasynaptic clusters of scaffolding proteins, i.e., SAP102 and PSD-95, have been previously described (Rao et al., 1998; Sans et al., 2000). However, a fraction of extrasynaptic receptors remains immobile in Stargazin ΔC-expressing neurons, suggesting stabilization by other mechanisms. Finally, due to the high level of fluorescence along neurites in Homer 1c::TdimerDsRed-expressing neurons, it is possible that we did not detect the dimmest clusters. Thus, some of the immobile "extrasynaptic" receptors could be actually localized on such clusters.

## Possible Models for Surface AMPAR-Stargazin Trafficking

Altogether, these results suggest a model in which concentration of AMPARs at postsynaptic sites is envisioned as a dynamic interplay between diffusing AMPARs and stabilization slots located below the plasma membrane. Our FRAP data show that AMPAR and Stargazin are associated at both synaptic and extrasynaptic sites, suggesting that they form stable complexes that can freely diffuse within the plasma membrane when not stabilized through binding to PSD-95. This is consistent with the idea that Stargazin is a constitutive AMPAR auxiliary subunit (Fukata et al., 2005; Vandenberghe et al., 2005b) that binds AMPARs early in the synthetic pathway and is required for AMPAR trafficking to the surface (Chen et al., 2000). However, the remaining fluorescence recovery observed during our experiments suggests that a small fraction of Stargazin can diffuse alone in the neuronal membrane. In support of this observation, biochemical data have shown that the interaction between TARP proteins and AMPARs can be disrupted by glutamate (Tomita et al., 2004), demonstrating that under certain conditions AMPARs and Stargazin can be trafficked independently.

Unbinding of AMPARs from the postsynaptic density and their subsequent increased diffusion could arise

either from disruption of the Stargazin-PSD-95 link or unbinding of a putative AMPAR/Stargazin/PSD-95 complex from another anchor. This other anchor could be PSD-95 itself or yet another PSD-95 synaptic partner. Indeed, PSD-95 can homomerize in an activity-dependent regulated manner (Christopherson et al., 2003; El-Husseini Ael et al., 2002). Our data cannot directly distinguish between these different possibilities. However, PSD-95 has a rather slow turnover at synapses, in the order of 25% over 5 min (Okabe et al., 2001; Sharma et al., 2006), a value which is much slower than the one we found for Stargazin (25% in 30 s). This suggests that the reversible link that allows AMPARs to traffic in and out synapses is mostly the Stargazin-PSD-95 interaction.

Finally, the regulation of the interaction between TARPs and associated MAGUKs and the subsequent changes in AMPAR surface trafficking, are likely to play a critical role in maturation and plasticity processes. On the one hand, the instability of AMPA signaling in immature synapses (Groc et al., 2006) parallels a low expression level of PSD-95/93, that substantially increase over development (Sans et al., 2000). Accordingly, we observed that the developmental decrease in AMPARs synaptic mobility is largely reversed by Stargazin ΔC expression. This could suggest that the interaction of Stargazin with SAP102 and then with increasing level of PSD-95/93 is involved in the higher trapping efficiency of AMPAR at mature synapses. On the other hand, Stargazin interaction with PSD-95 can be modulated by phosphorylation (Chetkovich et al., 2002). The PKA phosphorylation of Stargazin C terminus prevents Stargazin binding to PSD-95 (Chetkovich et al., 2002). Furthermore, Stargazin Cter tail is quantitatively phosphorylated on a set of serine residues. Phosphorylation and dephosphorylation of Stargazin are regulated by NMDAR activity and necessary for LTP and LTD of hippocampal synaptic transmission, respectively (Tomita et al., 2005). It will be of interest to determine how these processes regulate AMPARs surface trafficking to and from synapses.

## EXPERIMENTAL PROCEDURES

### Plasmid Constructs

GluR1 and GluR2 subunits were N-terminally epitope-tagged with an HA tag or a Myc tag, respectively. eGFP was inserted into Stargazin WT and mutants constructs between residues 269 and 270, at the BglII site. In Stargazin ΔC::GFP, the final four amino acids of Stargazin were deleted (Chen et al., 2000). For the Stargazin/PSD95 compensatory mutants (Schnell et al., 2002), the −2 position threonine of Stargazin was mutated to phenylalanine (StargazinT321F::GFP) and the 225 position histidine of PSD-95 was mutated to valine (PSD-95H221V). Wild-type PSD-95 was either unlabeled or C-terminally tagged with eGFP. For Homer 1c::TdimerDsRed, Homer 1c cDNA was subcloned into the eukaryotic expression vector pcDNA3 (Invitrogen) at the EcoRI sites, and TdimerDsRed was inserted N-terminally to the Homer 1c sequence between the Hind III/EcoRI sites. TdimerDsRed is a tandem dimer of the monomeric form of DsRed (Campbell et al., 2002). As a control for FRAP experiments, we used a construct comprising the transmembrane domain of NrCAM linked to an extracellular GFP, NrCAM-TM::GFP (Falk et al., 2004). Finally, the GluR2 ΔC::GFP construct was made by adding a stop codon before the last four amino acids of the GluR2 coding sequence using directed mutagenesis (QuickChange II XL Site-Directed Mutagenesis Kit, Stratagene). R2Delta4-F 5′-C GTA TAT GGC ATC GAG TGA GTT AAC ATT TAG GGG ATG ACC-3′ and R2Delta4-R 5′-GGT CAT CCC CTA AAT GTT AAC TCA CTC GAT GCC ATA TAC G-3′ were used as sense and antisense primers. Note that an HpaI site was inserted to screen the mutated clones. Plasmids were expressed by transient transfection in primary hippocampal cultures (see Supplemental Experimental Procedures).

### AMPAR and Stargazin Live Staining, QD-Based Tracking, FRAP Experiments, and Electrophysiological Recordings

Neurons were incubated 10 min with polyclonal anti-GluR1 (0.5 μg/ml, provided by Dr. Richard Huganir) or monoclonal anti-GluR2 (5 μg/ml, BD Pharmingen) at 37°C for the surface staining of GluR1-containing or GluR2-containing native AMPARs. GluR1::HA and Stargazin::HA were detected with a monoclonal anti-HA (0.5 μg/ml, Boehringer Mannheim) following the same procedure. Finally, extracellularly GFP-tagged GluR2 were immunostained using a monoclonal anti-GFP (0.5 μg/ml, Molecular Probes). After incubation with the primary antibody, neurons were washed and incubated 1 min at room temperature with Qdot 655 F(ab′)2 anti-rabbit or mouse IgG conjugate (2 nM, Quantum Dot corporation, Ozyme, France). After fast rinses, the coverslips were mounted in a custom chamber with culture medium supplemented with 20 mM HEPES. Neurons were imaged at 37°C on an inverted microscope (Olympus IX70; Olympus) equipped with a 100× oil-immersion objective (NA = 1.4). Samples were illuminated by a mercury lamp (Olympus). GFP, DsRed, and QDs were detected by using appropriate excitation filters (respectively, HQ480/20, HQ 565/20, and BP 420-480) and emission filters (respectively, 525/50, BA 590, and 655WB20). One thousand consecutive frames were acquired at 14 Hz with a CCD camera (CoolSnap HQ, Roper Scientific). All data were taken within 20 min after the last rinse of the coverslip. For FRAP experiments, 15–20 DIV hippocampal neurons were cotransfected with Stargazin::GFP and GluR2::TdimerDsRed (extracellular N-terminal tag) or NrCAM-TM::GFP and GluR2::TdimerDsRed. Experiments were performed either in control condition or after specific GluR2 crosslinking using sequential 10 min incubations with anti-DsRed antibodies (BD Pharmingen, 1/100) and Cy5- coupled secondary anti-mouse-IgGs (20 μg/ml, Jackson Immunoresearch Laboratories). See Supplemental Experimental Procedures for detail on fluorescence measurements and electrophysiological experiments.

### Trajectory Analysis

QDs exhibit random blinking; these dark periods are the signature of single QD but they prevent continuous tracking of the receptor. Single QD trajectories were constructed using homemade software. Trajectories obtained from one QD between the dark periods were connected only if the duration of the fluorescence disappearance and the distance covered by the particle during this period were under a threshold we defined (maximum distance from three to eight pixels and maximum blinks 200 frames). These thresholds have been adapted for each movie, according to the duration of the dark periods and the density of QDs in the field, to avoid the generation of more than one trajectory per QD or the connection between trajectories belonging to different QDs. Instantaneous diffusion coefficients, D, were calculated from linear fits of the n = 1 to 6 values of the mean squared displacement curves versus time using MSD (t) = $<r^2>$ (t) = 4Dt. For each trajectory, confined and diffusive periods were precisely detected as previously (Serge et al., 2002) using a mathematical function termed L function. This function is an index of the probability that a given time point belongs to a period in which the receptor remains in a membrane subregion for a duration longer than a Brownian diffusing (D = 0.2 $\mu m^2/s$) would stay in an equally sized region.

### GluR2 WT::GFP and GluR2 ΔC::GFP Surface Immunostaining

Neurons expressing either GluR2 WT::GFP or GluR2 ΔC::GFP were fixed with 4% paraformaldehyde and sucrose and washed with PBS and BSA. Fixed neurons were then incubated 20 min at room temperature with an anti-GFP polyclonal antibody (0.5 μg/ml, Molecular Probes). The primary antibodies were then revealed with Cy5-coupled anti-rabbit IgG secondary antibodies (4 μg/ml, Jackson Immunoresearch Laboratories) 30 min at room temperature. Coverslips were then mounted in Vectashield mounting medium. Images were acquired at the same exposure time using a Quantix digital cooled CCD camera (Photometric), and fluorescence levels were measured using Metamorph software (Universal Imaging).

### Statistical Analyses

Student's t test was used to test differences in mEPSC frequency and amplitude between groups in electrophysiology experiments and to test the difference in GluR2 surface expression between neurons transfected with either GluR2 WT::GFP or GluR2 ΔC::GFP. For the single particle tracking and FRAP experiments, differences in percentage of immobile receptor, in percentage of time confined, and half decay times were tested using Student's t test. Differences in median diffusion of mobile receptors were tested using Mann-Whitney test.

### Supplemental Data

The Supplemental Data for this article can be found online at http://www.neuron.org/cgi/content/full/53/5/719/DC1/.

## ACKNOWLEDGMENTS

We thank R.A. Nicoll and D.S. Bredt for providing Stargazin constructs, R.L. Huganir for providing GluR1 antibodies, S. El Mestikawy for providing the v-Glut1 antibodies, R. Tsien for the TdimerDsRed cDNA, V. Racine and J.B. Sibarita from the imaging center at the Curie Institute for providing the MIA software and helpful support, C. Poujol and P. Legros from the PICIN imaging center of Bordeaux for their continuous help, C. Breillat and A. Vimeney for precious help in performing molecular biology and cell culture work, and Laurent Cognet for help with data analysis. This work was supported by grants from the Centre National de la Recherche Scientifique, the Conseil Régional d'Aquitaine, the Ministère de la Recherche, the Fondation pour la Recherche Médicale, the Association Française contre les Myopathies, the Human Frontier Science Organisation, and the European Community Grants QLG3-CT-2001-02089 and CT-2005-005320.

Received: June 15, 2006
Revised: December 11, 2006
Accepted: January 26, 2007
Published: February 28, 2007

## REFERENCES

Adesnik, H., Nicoll, R.A., and England, P.M. (2005). Photoinactivation of native AMPA receptors reveals their real-time trafficking. Neuron *48*, 977–985.

Andrasfalvy, B.K., and Magee, J.C. (2004). Changes in AMPA receptor currents following LTP induction on rat CA1 pyramidal neurones. J. Physiol. *559*, 543–554.

Ashby, M.C., Maier, S.R., Nishimune, A., and Henley, J.M. (2006). Lateral diffusion drives constitutive exchange of AMPA receptors at dendritic spines and is regulated by spine morphology. J. Neurosci. *26*, 7046–7055.

Barry, M.F., and Ziff, E.B. (2002). Receptor trafficking and the plasticity of excitatory synapses. Curr. Opin. Neurobiol. *12*, 279–286.

Baude, A., Nusser, Z., Molnar, E., McIlhinney, R.A., and Somogyi, P. (1995). High-resolution immunogold localization of AMPA type glutamate receptor subunits at synaptic and non-synaptic sites in rat hippocampus. Neuroscience *69*, 1031–1055.

Beique, J.C., and Andrade, R. (2003). PSD-95 regulates synaptic transmission and plasticity in rat cerebral cortex. J. Physiol. *546*, 859–867.

Beique, J.C., Lin, D.T., Kang, M.G., Aizawa, H., Takamiya, K., and Huganir, R.L. (2006). Synapse-specific regulation of AMPA receptor function by PSD-95. Proc. Natl. Acad. Sci. USA *103*, 19535–19540.

Blanpied, T.A., Scott, D.B., and Ehlers, M.D. (2002). Dynamics and regulation of clathrin coats at specialized endocytic zones of dendrites and spines. Neuron *36*, 435–449.

Borgdorff, A.J., and Choquet, D. (2002). Regulation of AMPA receptor lateral movements. Nature *417*, 649–653.

Braithwaite, S.P., Meyer, G., and Henley, J.M. (2000). Interactions between AMPA receptors and intracellular proteins. Neuropharmacology *39*, 919–930.

Bredt, D.S., and Nicoll, R.A. (2003). AMPA receptor trafficking at excitatory synapses. Neuron *40*, 361–379.

Campbell, R.E., Tour, O., Palmer, A.E., Steinbach, P.A., Baird, G.S., Zacharias, D.A., and Tsien, R.Y. (2002). A monomeric red fluorescent protein. Proc. Natl. Acad. Sci. USA *99*, 7877–7882.

Chen, L., Chetkovich, D.M., Petralia, R.S., Sweeney, N.T., Kawasaki, Y., Wenthold, R.J., Bredt, D.S., and Nicoll, R.A. (2000). Stargazin regulates synaptic targeting of AMPA receptors by two distinct mechanisms. Nature *408*, 936–943.

Chetkovich, D.M., Chen, L., Stocker, T.J., Nicoll, R.A., and Bredt, D.S. (2002). Phosphorylation of the postsynaptic density-95 (PSD-95)/discs large/zona occludens-1 binding site of stargazin regulates binding to PSD-95 and synaptic targeting of AMPA receptors. J. Neurosci. *22*, 5791–5796.

Choquet, D., and Triller, A. (2003). The role of receptor diffusion in the organization of the postsynaptic membrane. Nat. Rev. Neurosci. *4*, 251–265.

Christopherson, K.S., Sweeney, N.T., Craven, S.E., Kang, R., El-Husseini Ael, D., and Bredt, D.S. (2003). Lipid- and protein-mediated multimerization of PSD-95: implications for receptor clustering and assembly of synaptic protein networks. J. Cell Sci. *116*, 3213–3219.

Chung, H.J., Xia, J., Scannevin, R.H., Zhang, X., and Huganir, R.L. (2000). Phosphorylation of the AMPA receptor subunit GluR2 differentially regulates its interaction with PDZ domain-containing proteins. J. Neurosci. *20*, 7258–7267.

Cognet, L., Groc, L., Lounis, B., and Choquet, D. (2006). Multiple routes for glutamate receptor trafficking: surface diffusion and membrane traffic cooperate to bring receptors to synapses. Sci. STKE *2006*, pe13.

Collingridge, G.L., Isaac, J.T., and Wang, Y.T. (2004). Receptor trafficking and synaptic plasticity. Nat. Rev. Neurosci. *5*, 952–962.

Cottrell, J.R., Dube, G.R., Egles, C., and Liu, G. (2000). Distribution, density, and clustering of functional glutamate receptors before and after synaptogenesis in hippocampal neurons. J. Neurophysiol. *84*, 1573–1587.

Dahan, M., Levi, S., Luccardini, C., Rostaing, P., Riveau, B., and Triller, A. (2003). Diffusion dynamics of glycine receptors revealed by single-quantum dot tracking. Science *302*, 442–445.

Dakoji, S., Tomita, S., Karimzadegan, S., Nicoll, R.A., and Bredt, D.S. (2003). Interaction of transmembrane AMPA receptor regulatory proteins with multiple membrane associated guanylate kinases. Neuropharmacology *45*, 849–856.

Daw, M.I., Chittajallu, R., Bortolotto, Z.A., Dev, K.K., Duprat, F., Henley, J.M., Collingridge, G.L., and Isaac, J.T. (2000). PDZ proteins interacting with C-terminal GluR2/3 are involved in a PKC-dependent regulation of AMPA receptors at hippocampal synapses. Neuron *28*, 873–886.

DeSouza, S., Fu, J., States, B.A., and Ziff, E.B. (2002). Differential palmitoylation directs the AMPA receptor-binding protein ABP to spines or to intracellular clusters. J. Neurosci. *22*, 3493–3503.

Dingledine, R., Borges, K., Bowie, D., and Traynelis, S.F. (1999). The glutamate receptor ion channels. Pharmacol. Rev. *51*, 7–61.

Ehrlich, I., and Malinow, R. (2004). Postsynaptic density 95 controls AMPA receptor incorporation during long-term potentiation and experience-driven synaptic plasticity. J. Neurosci. *24*, 916–927.

El-Husseini, A.E., Schnell, E., Chetkovich, D.M., Nicoll, R.A., and Bredt, D.S. (2000). PSD-95 involvement in maturation of excitatory synapses. Science *290*, 1364–1368.

El-Husseini Ael, D., Schnell, E., Dakoji, S., Sweeney, N., Zhou, Q., Prange, O., Gauthier-Campbell, C., Aguilera-Moreno, A., Nicoll, R.A., and Bredt, D.S. (2002). Synaptic strength regulated by palmitate cycling on PSD-95. Cell *108*, 849–863.

Elias, G.M., Funke, L., Stein, V., Grant, S.G., Bredt, D.S., and Nicoll, R.A. (2006). Synapse-specific and developmentally regulated targeting of AMPA receptors by a family of MAGUK scaffolding proteins. Neuron *52*, 307–320.

Falk, J., Thoumine, O., Dequidt, C., Choquet, D., and Faivre-Sarrailh, C. (2004). NrCAM coupling to the cytoskeleton depends on multiple protein domains and partitioning into lipid rafts. Mol. Biol. Cell *15*, 4695–4709.

Fukata, Y., Tzingounis, A.V., Trinidad, J.C., Fukata, M., Burlingame, A.L., Nicoll, R.A., and Bredt, D.S. (2005). Molecular constituents of neuronal AMPA receptors. J. Cell Biol. *169*, 399–404.

Garner, C.C., Nash, J., and Huganir, R.L. (2000). PDZ domains in synapse assembly and signalling. Trends Cell Biol. *10*, 274–280.

Garner, C.C., Zhai, R.G., Gundelfinger, E.D., and Ziv, N.E. (2002). Molecular mechanisms of CNS synaptogenesis. Trends Neurosci. *25*, 243–251.

Groc, L., Heine, M., Cognet, L., Brickley, K., Stephenson, F.A., Lounis, B., and Choquet, D. (2004). Differential activity-dependent regulation of the lateral mobilities of AMPA and NMDA receptors. Nat. Neurosci. *7*, 695–696.

Groc, L., Gustafsson, B., and Hanse, E. (2006). AMPA signalling in nascent glutamatergic synapses: there and not there! Trends Neurosci. *29*, 132–139.

Hollmann, M., and Heinemann, S. (1994). Cloned glutamate receptors. Annu. Rev. Neurosci. *17*, 31–108.

Howarth, M., Takao, K., Hayashi, Y., and Ting, A.Y. (2005). Targeting quantum dots to surface proteins in living cells with biotin ligase. Proc. Natl. Acad. Sci. USA *102*, 7583–7588.

Keinanen, K., Wisden, W., Sommer, B., Werner, P., Herb, A., Verdoorn, T.A., Sakmann, B., and Seeburg, P.H. (1990). A family of AMPA-selective glutamate receptors. Science *249*, 556–560.

Kim, E., and Sheng, M. (2004). PDZ domain proteins of synapses. Nat. Rev. Neurosci. *5*, 771–781.

Kim, C.H., Chung, H.J., Lee, H.K., and Huganir, R.L. (2001). Interaction of the AMPA receptor subunit GluR2/3 with PDZ domains regulates hippocampal long-term depression. Proc. Natl. Acad. Sci. USA *98*, 11725–11730.

Kusumi, A., Sako, Y., and Yamamoto, M. (1993). Confined lateral diffusion of membrane receptors as studied by single particle tracking (nanovid microscopy). Effects of calcium-induced differentiation in cultured epithelial cells. Biophys. J. *65*, 2021–2040.

Kusumi, A., Nakada, C., Ritchie, K., Murase, K., Suzuki, K., Murakoshi, H., Kasai, R.S., Kondo, J., and Fujiwara, T. (2005). Paradigm shift of the plasma membrane concept from the two-dimensional continuum fluid to the partitioned fluid: high-speed single-molecule tracking of membrane molecules. Annu. Rev. Biophys. Biomol. Struct. *34*, 351–378.

Malinow, R., and Malenka, R.C. (2002). AMPA receptor trafficking and synaptic plasticity. Annu. Rev. Neurosci. *25*, 103–126.

Meier, J., Vannier, C., Serge, A., Triller, A., and Choquet, D. (2001). Fast and reversible trapping of surface glycine receptors by gephyrin. Nat. Neurosci. *4*, 253–260.

Migaud, M., Charlesworth, P., Dempster, M., Webster, L.C., Watabe, A.M., Makhinson, M., He, Y., Ramsay, M.F., Morris, R.G., Morrison, J.H., et al. (1998). Enhanced long-term potentiation and impaired learning in mice with mutant postsynaptic density-95 protein. Nature *396*, 433–439.

Nicoll, R.A., Tomita, S., and Bredt, D.S. (2006). Auxiliary subunits assist AMPA-type glutamate receptors. Science *311*, 1253–1256.

Nusser, Z., Lujan, R., Laube, G., Roberts, J.D., Molnar, E., and Somogyi, P. (1998). Cell type and pathway dependence of synaptic AMPA receptor number and variability in the hippocampus. Neuron *21*, 545–559.

O'Brien, R.J., Lau, L.F., and Huganir, R.L. (1998). Molecular mechanisms of glutamate receptor clustering at excitatory synapses. Curr. Opin. Neurobiol. *8*, 364–369.

O'Brien, R.J., Xu, D., Petralia, R.S., Steward, O., Huganir, R.L., and Worley, P. (1999). Synaptic clustering of AMPA receptors by the extracellular immediate-early gene product Narp. Neuron *23*, 309–323.

O'Brien, R., Xu, D., Mi, R., Tang, X., Hopf, C., and Worley, P. (2002). Synaptically targeted narp plays an essential role in the aggregation of AMPA receptors at excitatory synapses in cultured spinal neurons. J. Neurosci. *22*, 4487–4498.

Okabe, S., Urushido, T., Konno, D., Okado, H., and Sobue, K. (2001). Rapid redistribution of the postsynaptic density protein PSD-Zip45 (Homer 1c) and its differential regulation by NMDA receptors and calcium channels. J. Neurosci. *21*, 9561–9571.

Osten, P., Khatri, L., Perez, J.L., Kohr, G., Giese, G., Daly, C., Schulz, T.W., Wensky, A., Lee, L.M., and Ziff, E.B. (2000). Mutagenesis reveals a role for ABP/GRIP binding to GluR2 in synaptic surface accumulation of the AMPA receptor. Neuron *27*, 313–325.

Passafaro, M., Piech, V., and Sheng, M. (2001). Subunit-specific temporal and spatial patterns of AMPA receptor exocytosis in hippocampal neurons. Nat. Neurosci. *4*, 917–926.

Perez, J.L., Khatri, L., Chang, C., Srivastava, S., Osten, P., and Ziff, E.B. (2001). PICK1 targets activated protein kinase Calpha to AMPA receptor clusters in spines of hippocampal neurons and reduces surface levels of the AMPA-type glutamate receptor subunit 2. J. Neurosci. *21*, 5417–5428.

Racz, B., Blanpied, T.A., Ehlers, M.D., and Weinberg, R.J. (2004). Lateral organization of endocytic machinery in dendritic spines. Nat. Neurosci. *7*, 917–918.

Rao, A., Kim, E., Sheng, M., and Craig, A.M. (1998). Heterogeneity in the molecular composition of excitatory postsynaptic sites during development of hippocampal neurons in culture. J. Neurosci. *18*, 1217–1229.

Rouach, N., Byrd, K., Petralia, R.S., Elias, G.M., Adesnik, H., Tomita, S., Karimzadegan, S., Kealey, C., Bredt, D.S., and Nicoll, R.A. (2005). TARP gamma-8 controls hippocampal AMPA receptor number, distribution and synaptic plasticity. Nat. Neurosci. *8*, 1525–1533.

Sans, N., Petralia, R.S., Wang, Y.X., Blahos, J., 2nd, Hell, J.W., and Wenthold, R.J. (2000). A developmental change in NMDA receptor-associated proteins at hippocampal synapses. J. Neurosci. *20*, 1260–1271.

Scannevin, R.H., and Huganir, R.L. (2000). Postsynaptic organization and regulation of excitatory synapses. Nat. Rev. Neurosci. *1*, 133–141.

Schnell, E., Sizemore, M., Karimzadegan, S., Chen, L., Bredt, D.S., and Nicoll, R.A. (2002). Direct interactions between PSD-95 and stargazin control synaptic AMPA receptor number. Proc. Natl. Acad. Sci. USA *99*, 13902–13907.

Seidenman, K.J., Steinberg, J.P., Huganir, R., and Malinow, R. (2003). Glutamate receptor subunit 2 Serine 880 phosphorylation modulates

synaptic transmission and mediates plasticity in CA1 pyramidal cells. J. Neurosci. *23*, 9220–9228.

Serge, A., Fourgeaud, L., Hemar, A., and Choquet, D. (2002). Receptor activation and homer differentially control the lateral mobility of metabotropic glutamate receptor 5 in the neuronal membrane. J. Neurosci. *22*, 3910–3920.

Sharma, K., Fong, D.K., and Craig, A.M. (2006). Postsynaptic protein mobility in dendritic spines: long-term regulation by synaptic NMDA receptor activation. Mol. Cell. Neurosci. *31*, 702–712.

Sheng, M. (2001). Molecular organization of the postsynaptic specialization. Proc. Natl. Acad. Sci. USA *98*, 7058–7061.

Song, I., and Huganir, R.L. (2002). Regulation of AMPA receptors during synaptic plasticity. Trends Neurosci. *25*, 578–588.

Stein, V., House, D.R., Bredt, D.S., and Nicoll, R.A. (2003). Postsynaptic density-95 mimics and occludes hippocampal long-term potentiation and enhances long-term depression. J. Neurosci. *23*, 5503–5506.

Tardin, C., Cognet, L., Bats, C., Lounis, B., and Choquet, D. (2003). Direct imaging of lateral movements of AMPA receptors inside synapses. EMBO J. *22*, 4656–4665.

Terashima, A., Cotton, L., Dev, K.K., Meyer, G., Zaman, S., Duprat, F., Henley, J.M., Collingridge, G.L., and Isaac, J.T. (2004). Regulation of synaptic strength and AMPA receptor subunit composition by PICK1. J. Neurosci. *24*, 5381–5390.

Tomita, S., Chen, L., Kawasaki, Y., Petralia, R.S., Wenthold, R.J., Nicoll, R.A., and Bredt, D.S. (2003). Functional studies and distribution define a family of transmembrane AMPA receptor regulatory proteins. J. Cell Biol. *161*, 805–816.

Tomita, S., Fukata, M., Nicoll, R.A., and Bredt, D.S. (2004). Dynamic interaction of stargazin-like TARPs with cycling AMPA receptors at synapses. Science *303*, 1508–1511.

Tomita, S., Stein, V., Stocker, T.J., Nicoll, R.A., and Bredt, D.S. (2005). Bidirectional synaptic plasticity regulated by phosphorylation of stargazin-like TARPs. Neuron *45*, 269–277.

Triller, A., and Choquet, D. (2003). Synaptic structure and diffusion dynamics of synaptic receptors. Biol. Cell. *95*, 465–476.

Vandenberghe, W., Nicoll, R.A., and Bredt, D.S. (2005a). Interaction with the unfolded protein response reveals a role for stargazin in biosynthetic AMPA receptor transport. J. Neurosci. *25*, 1095–1102.

Vandenberghe, W., Nicoll, R.A., and Bredt, D.S. (2005b). Stargazin is an AMPA receptor auxiliary subunit. Proc. Natl. Acad. Sci. USA *102*, 485–490.

Xu, D., Hopf, C., Reddy, R., Cho, R.W., Guo, L., Lanahan, A., Petralia, R.S., Wenthold, R.J., O'Brien, R.J., and Worley, P. (2003). Narp and NP1 form heterocomplexes that function in developmental and activity-dependent synaptic plasticity. Neuron *39*, 513–528.